Advanced Powder Technology 26 (2015) 742–752

Contents lists available at ScienceDirect

Advanced Powder Technology

journal homepage: www.elsevier.com/locate/apt

Original Research Paper

Numerical modelling of the normal adhesive elastic–plastic interaction of a bacterium

Raimondas Jasevičius [a,b,*], Romas Baronas [b], Harald Kruggel-Emden [c]

[a] Institute of Mechanical Science, Vilnius Gediminas Technical University, Vilnius, Lithuania
[b] Department of Software Engineering, Vilnius University, Vilnius, Lithuania
[c] Department of Energy Plant Technology, Ruhr-Universität Bochum, Bochum, Germany

ARTICLE INFO

Article history:
Received 30 September 2014
Received in revised form 17 March 2015
Accepted 17 April 2015
Available online 25 April 2015

Keywords:
Staphylococcus aureus
Bacterium
Elastic–plastic deformation
DLVO model
Discrete element method

ABSTRACT

Bacteria are a widespread group of organisms. On the microscale, bacteria colonies are of discrete nature. Looking from the mechanical point of view the suspension containing the bacteria may be considered as a system of living active ultrafine particles (size: 0.1–10 μm). In order to understand the mechanical behaviour of the bacteria system it is important to understand the behaviour of a single bacterium. The present paper proposes an adhesive interaction model for the simulation of bacteria cells, which can be also applied for the interaction for other biological cells. The main attention is given to describe and numericaly simulate the interaction of a bacterium with a flat surface within a liquid medium. In the simulations an adhesive force is taken into account. Adhesion plays a significant role, because it can keep a bacterium on the surface. It is described by the attractive van der Waals force. In order to achieve the stick of adhesive particles, additionally developed adhesive–dissipative models are presented. The bacterium interaction is described by an elastic–plastic model; these results are thereafter compared with results from an elastic model. Different known models such as Derjaguin, Müller and Toporov (DMT) and Derjaguin, Landau, Verwey, Overbeek (DLVO) models are considered. Obtained results show the approach and deformation process of an adhesive–dissipative bacterium by presenting force displacement diagrams. The bacterium–surface interaction model is developed in the framework of the discrete element method (DEM). The numerical experiments confirm that force–displacement plots exhibit a hysteresis similar to those observed in Atomic Force Microscopy (AFM) experiments. The proposed model can be applied for the numerical simulation of the interaction process of bacteria with a surface, as well as simulations of the sticking process.

1. Introduction

Human sneezing, coughing, as well as the operation of devices such as humidifiers and air conditioning systems are a reason for bacteria motion which can trigger the spread of infectious agents. The motion of bacteria can be interpreted as the motion of micron sized particles. Usually bacteria are contained within small droplets forming an aerosol. The transmission of this aerosol was investigated by Tang et al. [1] as well as Todd and Belteton [2]. In order to understand the bacterium behaviour during spreading, the bacterium interaction shifts into the main focus. Thereby, different approaches can be applied for the simulation of bacteria motion.

The bacterium interaction is governed by numerous natural external forces which make bacteria movement different to that of non-living bodies looking from a classical mechanics point of view. Nonetheless, the movement is governed by attractive and repulsive forces. The simulation of ultrafine sized interacting objects can be described by applying the Derjaguin, Landau, Verwey, Overbeek (DLVO) model [3–6]. That the DLVO theory is also valid for microbial adhesion was observed by Hermansson [7], Azeredo et al. [8]. The latter DLVO model includes attractive adhesive and repulsive electrostatic double-layer forces, which act at a distance of interacting surfaces.

An important role for the bacterium interaction plays adhesion, which can be a reason for sticking. Usually adhesion is described by attractive van der Waals forces. A review of mechanisms of

* Corresponding author at: Institute of Mechanical Science, Vilnius Gediminas Technical University, Vilnius, Lithuania.
E-mail address: raimondas.jasevicius@vgtu.lt (R. Jasevičius).

http://dx.doi.org/10.1016/j.apt.2015.04.010
0921-8831/

bacterial adhesion to biomaterial surfaces was performed by An and Friedman [9]. The stick of *Staphylococcus aureus* to mucus components of the respiratory epithelium was investigated by Ulrich et al. [10]. The influence of adhesion can be also observed for the spores (Zhao et al. [11]). Adhesion to titanium surfaces of *S. aureus* bacteria was investigated by Harris and Richards [12]. Different surface roughnesses of the bacterium and of the substrate can be a reason for the change of the van der Waals force. The roughness of bacteria was therefore analysed by Francius et al. [13]. *S. aureus* attachment patterns on glass surfaces with nanoscale roughness were investigated by Mitik-Dineva et al. [14].

The influence of attractive forces can be a reason for the formation of bacterial structures such as biofilms. Biofilm formation basing on adhesive interaction was investigated by Cramton et al. [15]. Mechanisms of biofilm structure formation in *Staphylococcus* bacteria were investigated by Mack et al. [16] and Ha et al. [17]. The influence of repulsion forces between interacting surfaces at a distance reduces the probability of attraction and stick to a surface. In this context the influence of electric double layers in bacterial adhesion to surfaces was investigated by Poortinga et al. [18]. The existence of a force–displacement hysteresis was observed from physical experiments with bacteria provided by the means of the atomic force microscopy (AFM) by Ubbink and Schär-Zammaretti [19]. Atomic force microscopy of microbial cells was performed by Butt et al. [20] and Gaboriaud and Dufrêne [21]. Abu-Lail and Camesano [22] investigated the elasticity and molecular surface characteristics of *Escherichia Coli* via atomic force microscopy (AFM). The Hertz theory is used not only for microparticles or nanoparticles, but is taken into account also for bioparticles such as cells (comp. Lulevich et al. [23] and Gaboriaud and Dufrêne [21]). However, as bacteria are non-homogenous, it is difficult to describe the deformation only with the nonlinear elastic Hertz model, see Butt et al. [20]. The indentation of living cells by interpretation of AFM experimental data is a difficult task, because it can be governed by various properties, such as plastic and elastic behaviour, viscosity and adhesion, see Sirghi [24]. Therefore, the reason to investigate the elastic–plastic behaviour of bacteria in a numerical framework is of high relevance. Following this idea the comparison of elastic and elastic–plastic contact behaviour is presented below. Plastic deformation of a *Staphylococcus epidermidis* bacterium was observed by Méndez-Vilas et al. [25]. Elastic–plastic behaviour of *Aspergillus nidulans* spores was observed by Zhao et al. [11] depending on the value of the applied load.

In this paper the main attention is given to the description and numerical simulation of the interaction of a bacterium with a flat surface surrounded by a liquid medium. Using a particle description for the bacterium interaction, the discrete element method (DEM) is used to resolve the interaction process.

2. Problem formulation

A pathogenic bacterium initially placed in an aerosol droplet (bioaerosol) has the ability to travel through the air and stick to various surfaces. Initially, as the bacterium is dispersed within the bioaerosol the bacterium motion depends on the bioaerosol droplet motion. In most cases, the behaviour of a bacterium during the contact is treated, however, in a non-unique way, and different models may be used in the numerical analysis. It should be noted that even the simplest adhesion process may be not only reversible; however, it can involve the adhesive dissipation of energy. Therefore, the enhancing of the knowledge of the mechanisms of the energy dissipation due to adhesion forces in the normal direction is the main task of the present paper.

In the performed analysis the motion of the bacterium is idealized and limited to the investigation of the interaction of a bacterium with a flat surface dispersed in a liquid medium. This approach must be understood as a first step towards more complex models including e.g. the motion of the liquid of a surrounding aerosol droplet. The chosen bacterium is the *Staphylococcus aureus* which is in many ways pathogenic. The bacterium-surface interaction mechanisms are not well understood, while different factors may influence the interaction [24]. The known DLVO model may describe bacterium interaction, when the interacting surfaces are at a certain distance within a liquid medium. The theoretical interpretation of the deformation behaviour of a bacterium during contact is still missing but required, as it is essential to understand the nature of the bacterium interaction.

In this analysis the bacterium is considered as a spherical particle. The interaction with the surface is described by normal force components. The attraction force between interacting surfaces is considered by van der Waals forces. Additionally short range interaction is taken into account, which is load dependent and related to the adhesion energy dissipation mechanism. Physical experiments with atomic force measurements (AFM) show that the *S. aureus* bacterium reveals dissipative contact behaviour, as force–displacement diagrams show a hysteretic behaviour of the bacterium, see Touhami et al. [26] and Abu-Lail et al. [27]. The objective of the work here is to describe the bacterium interaction by taking into account the adhesive–dissipative mechanism into the model. The goal of this work is the description and numerical analysis of the adhesive normal interaction of a bacterium with a surface by taking into account elastic and elastic–plastic mechanisms. The observed model is derived based on DLVO and DMT models for the description of the bacterium interaction. The DLVO model is usually used only for the description of the interaction without any contact deformation of colloid particles, while the DMT model describes contact of ultrafine particles. The theoretical basis for the bacteria movement is based on investigations of same size non-organic ultrafine particles, see Tomas [28] and Jasevičius et al. [29,30].

A description of the behaviour of a bacterium during interaction is necessary for which the energy dissipation needs to be correlated with the influence of the attraction. As a result this gives the ability to stick and structures like biofilms can be formed. Energy dissipation is presented as a mechanism, which depends on the amount of dissipated energy and is related to adhesion. A bacterium loses energy during the unloading and detachment process as it is expected for the deformation of micron sized objects (comp. Jasevičius et al. [29,30] and Jasevičius et al. [31,32]).

In order to describe the deformation process due to adhesion, two known adhesive elastic models the Derjaguin, Müller, Toporov (DMT) and the Johnson, Kendall, Roberts (JKR) approach are discussed. DMT and JKR models are usually used to describe the deformation of adhesive particles in normal direction and can be applied for the investigation of bacterium interaction. Initially DMT and JKR models were derived for non-biological particles, where the elastic deformation is based on the Hertz model. The DMT model is usually used for ultrafine particles, when particle diameters are less than 10 μm, while the JKR model is used for softer and larger particles. DMT and JKR models do not take into account the van der Waals influence during the interaction at a distance when interacting surfaces are not in contact. Furthermore, these models do not take force–displacement hysteresis effects related to adhesion, which are observed in experiments with AFM, into account. In fact both DMT and JKR models are not sufficient to describe the influence of adhesion on microsize objects during the sticking process, even when we investigate objects surrounded by a liquid. Note, that for ultrafine particles, the JKR model results in too little energy dissipation and therefore has its difficulties explaining experimental investigations, see Jasevičius et al. [30].

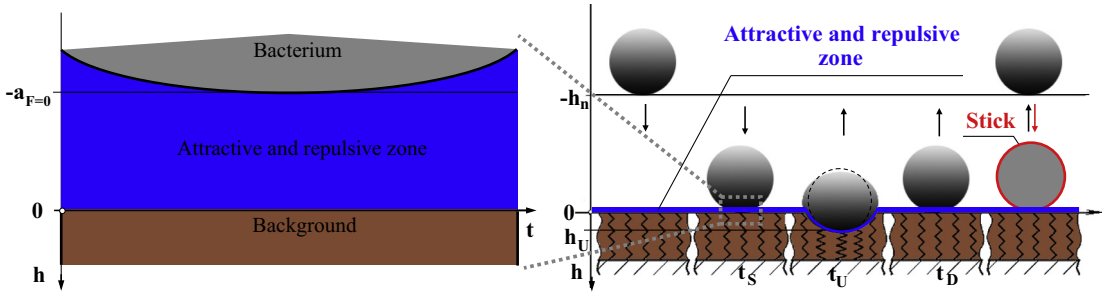

Fig. 1. Movement of a bacterium, during interaction with a flat surface.

We therefore use an interaction model, which is based on the DMT model for several reasons. It was developed to include energy dissipation mechanism related to adhesion for ultrafine size particles and is based on the DMT. The energy dissipation mechanism related to adhesion let us get enough energy for dissipation and let us also get a force–displacement hysteresis due to adhesion for bacteria as obtained in experiments with AFM. Otherwise for a better understanding of adhesive energy dissipation mechanism, coefficients of restitution and results on impact test are needed, while it is difficult to make such experiment with a bacterium, as a bacterium can rupture. Because of that, previous theoretical investigations of ultrafine particles become important for the understanding of the influence of adhesion. In this work a model for ultrafine particle interaction was implemented for a bacteria cell. Here the dissipation mechanisms are bacteria load dependent and related to the change of surface roughness and the van der Waals force during deformation. Contrary to this DMT and JKR models describe only the elastic particle behaviour and they are not originally suited for elastic–plastic deformation. We assumed that during bacterium soft interaction, adhesive elastic–plastic contact is prevailed.

As our bacterium is of a diameter of 1 μm and because we also want to take into account the energy dissipation related to adhesion and describe the elastic–plastic deformation and the bacterium sticking process, we use a model which is based on the DMT for ultrafine size particles. Otherwise the JKR model based on an additional elastic extension during unloading for softer particles is needed for the investigation. Also implemented and required would be an adhesion related energy dissipation mechanism which is independent of the initial velocity and considers the effect of a hysteresis to model for the attractive interaction at the distance with the JKR model for the simulation within the DEM. Finally not only normal, but also tangential interaction of a bacterium is important for simulations within the DEM. For ultrafine particles tangential interaction models can be found in [30,35] and can also be applied for the bacterium interaction.

Our other main task is to derive a model, which would include typical characteristic phenomena of a bacterium and can be applied to numerical simulations involving the discrete element method (DEM). In this work the model is adopted for DEM simulations, while DEM is also suitable for the simulation of different shaped particles (see e.g. Kruggel-Emden and Elskamp [33] or Kruggel-Emden and Oschmann [34]). In the present investigation the adhesive–dissipative model, which applies DEM, offers the opportunity to capture the dissipation effect during the contact and simulate the interaction of a bacterium with a substrate. A collision between a bacterium and a flat surface is mainly attributed to the attractive van der Waals, double layer electrostatic force and steric force. In order to compare different forms of deformation behaviour of a bacterium in this paper a comparison of dissipative adhesive elastic and elastic–plastic interactions is presented.

In most cases, the behaviour of a bacterium during contact is not fully understood and only limited knowledge is available in scientific literature. Therefore, the investigation addressing the nature of the bacterium interaction is of high relevance looking from the spread of an infection point of view. This task is analysed from a mechanical perspective.

3. Simulation methodology and basic relationships

3.1. Basic models

One of the models usually used to describe the behaviour of colloids and adopted also for the interaction of bacteria is the DLVO (Derjaguin, Landau, Verwey, and Overbeek) approach. The DLVO terms decay over a very short distance of 20 nm, see e.g. Camesano and Logan [36]. The DLVO model describes the interaction without any contact deformation.

Based on the DLVO theory the interaction between two bacteria without contact (approach or detachment) is assumed to consist of two contributions: the van der Waals attraction and electrostatic double-layer repulsion.

$$\boldsymbol{F}_{DLVO}(t) = \boldsymbol{F}_{dl}(t) + \boldsymbol{F}_{vdW}(t) \tag{1}$$

Here: $\boldsymbol{F}_{dl}$ – repulsive double layer electrostatic force; $\boldsymbol{F}_{vdW}$ – attractive van der Waals force.

The Derjaguin, Müller and Toporov (DMT) model takes into account particle behaviour during deformation (loading or unloading) and is used for fine and stiff particles. The deformation depends on attractive van der Waals forces and the repulsive elastic Hertz model:

$$\boldsymbol{F}_{DMT}(t) = \boldsymbol{F}_{Hertz}(t) + \boldsymbol{F}_{vdW} \tag{2}$$

Here: $\boldsymbol{F}_{Hertz}$ – repulsive elastic force, Hertz model; $\boldsymbol{F}_{vdW}$ – attractive van der Waals force, const.

The constitutive model for normal adhesive contact of a bacterium on plane substrate is formulated based on a combined DMT and DLVO model. These models involve the combined action of the repulsive contact and an attractive adhesive force. It should be noted that the elastic contact is an extreme case of a (stiff) deformable particle model, which will be applied to evaluate the upper bound of the contact behaviour of a bacterium.

The movement of a bacterium is presented in Fig. 1. Firstly, the bacterium, is moving from a certain distance h_n to a surface. The interaction starts at time instant t_S when the bacterium comes into the attractive and repulsive zone, presented in Fig. 1 by the blue[1] area. In this work we investigate only the interaction process and the time instance t_S is assumed to be the initial time $t_0 = 0$. The distance at which the interaction starts is described by the instance when force equilibrium at displacement $a_{F=0}$ is acting on the bacterium. Here the particle has reached a displacement $h < 0$. Attraction is related to the van der Waals force. When the particle

reaches the surface with displacement $h = 0$, the contact area of the interacting surfaces is under deformation and the overall process is described as loading with displacement $h > 0$. During the progression of the contact the interacting surfaces of the bacterium and the substrate reach a maximum overlap at time t_U and a reversal of the motion begins. After that the bacterium remains in the unloading process with displacement $h > 0$. During unloading, when the bacterium reaches a displacement distance of $h = 0$, the contact of the bacterium with the substrate ends. At time instance t_D the bacterium leaves the attractive and repulsive zone which is described as detachment with displacement $h < 0$. If the bacterium has not enough initial kinetic energy for rebound, the interaction continuous and the bacterium sticks to the flat surface of the substrate. Note that our investigation is limited to the bacterium interaction from time instance t_S till time instance t_D.

3.2. Simulation methodology

The discrete element method (DEM) based on Lagrangian approach and is applied to simulate the dynamic behaviour of the bacterium under normal impact. The bacteria are considered as adhesive ultrafine active particles. The motion of an arbitrary bacterium i in time t during normal contact is characterized by the global parameters: positions $\boldsymbol{x}_i$, velocities $\dot{\boldsymbol{x}}_i = \mathrm{d}\boldsymbol{x}_i/\mathrm{d}t$ and accelerations $\ddot{\boldsymbol{x}}_i = \mathrm{d}^2\boldsymbol{x}_i/\mathrm{d}t^2$ of the centre of mass and a force $\boldsymbol{F}_i$ applied to it. The global parameters are defined in Cartesian coordinates. Translational motion is described by the Newton's second law applied to each bacterium i:

$$m_i\ddot{\boldsymbol{x}}_i(t) = \boldsymbol{F}_i(t), \tag{3}$$

where m_i is the bacterium's mass. The resultant force acting on the bacterium may comprise of the prescribed as well as interaction and field forces. Consequently, for normal interaction, vector Eq. (3) reduces to a scalar equation, while the force vector reduces to a single normal force F_i^N. The methodology for the calculation of the interaction forces in Eq. (3) depends on the bacterium size, shape and mechanical properties as well as on the constitutive model of the interaction. The dynamical state of the bacterium during interaction is tracked in space and time by integration of Eq. (3). The numerical solution at time $t + \Delta t$ is obtained incrementally with constant time step Δt by using a 5th-order Gear predictor–corrector scheme. The discussed methodology was implemented into an in-house DEM code. The constitutive model for the normal adhesive contact of an ultrafine bacterium on a plane substrate is formulated based on known models. The model involves the combined action of the repulsive contact force and an attractive adhesive force.

The bacterium interaction is described based on known models by applying three different normal force components: attraction $\boldsymbol{F}^N_{attr}(t)$, repulsion $\boldsymbol{F}^N_{repulsion}(t)$ and dissipation $\boldsymbol{F}^N_{diss}(t)$. Generally the normal force of the bacterium interaction with a surface can be described as a sum of these forces:

$$\boldsymbol{F}^N(t) = \boldsymbol{F}^N_{repulsion}(t) + \boldsymbol{F}^N_{attr}(t) + \boldsymbol{F}^N_{diss}(t) \tag{4}$$

A different combination of these forces plays a significant role during the approach, loading, unloading and detachment of the bacterium. Now the movement of a bacterium will be introduced.

For the description of the bacterium behaviour we compare two different models. These models rely on different interpretations of the deformation process. With the first model contact is adhesive elastic dissipative and deformation is described with the time dependent elastic Hertz model. With the second model, it is assumed that contact is adhesive elastic–plastic dissipative. In both cases in the non-contact deformation zone, when interacting surfaces are at a distance, interaction is described in the same way, with time dependent attractive van der Waals, repulsive electrostatic double layer and steric forces. Hydrodynamic force is not considered here.

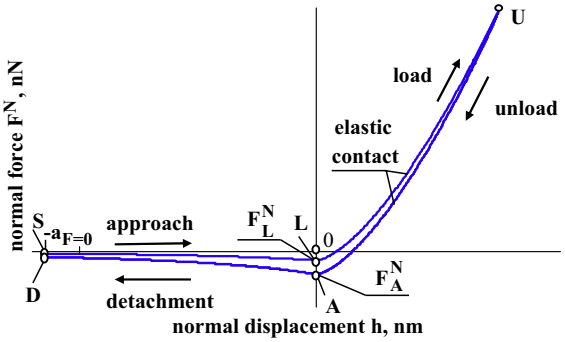

Fig. 2. The force–displacement diagram of the normal attractive elastic dissipative bacterium-plane contact. The bacterium approaches the plane surface, line S–L, Eq. (5), forms an elastic contact, line L–U, Eq. (13), and is unloaded at point U, line U–A, Eq. (21). Then it achieves the adhesion limit at point A and finally detaches, line A–D, Eq. (23). The required material data for this diagram, including characteristic parameters of adhesion, such as minimum distance $a_{F=0}$ and adhesion force $F^N_{L,adh}$, electrostatic double layer force F^N_{dl}, deformation of biological polymers on bacterium surface describing steric force F^N_{steric}, elasticity parameters, such as modulus of elasticity E and Poisson ratio ν, are given in the Basic Data section.

The considered models of the normal interaction are described in terms of a force–displacement relationship. If we define a normal orientation of the contact by a unit vector $\boldsymbol{N}$, the force vector $\boldsymbol{F}^N = F^N N$ may be described by the time-dependent scalar variable $F^N(t)$.

Four different stages may be distinguished during the normal interaction. They include: the non-contact approach, contact loading, contact unloading and non-contact detachment. When a bacterium moves towards the surface, the short range interaction is characterized as the approach, while the motion in the outward direction is characterized as detachment. The contact interaction comprises of loading and unloading. Four time-dependent components of the normal force are used in the description of the contact. The approach stage is characterized by the force $F^N_{appr}(t)$, the loading stage by $F^N_{load}(t)$, unloading by $F^N_{unload}(t)$ and the detachment stage by $F^N_{detach}(t)$, respectively.

3.3. Adhesive dissipative elastic interaction

The normal force–displacement diagram of the bacterium is modelled as for a particle. The constitutive interaction model may be illustrated by the diagram (S–L–U–A–D) of force $F^N \equiv F^N_i$ and displacement h plotted in Fig. 2. The model is restricted by the displacement as minimum separation distance $h = -a_{F=0}$. Here, the repulsive forces are defined as positive, while attractive forces by negative values. The negative displacement corresponds to the interaction with no contact and no deformation, whereas the positive displacement coincides with the interaction with contact when the bacterium deforms. Firstly, contact loading and unloading in opposite direction are shown by the arrows.

Fig. 2 presents a theoretical model for defining the normal interaction involving two parts. A negative displacement denotes to the left part of Fig. 2 and covers the bacterium approach (S–L) and detachment (A–D). A positive displacement takes place when the right part includes loading (L–U) and unloading (U–A).

The reversible behaviour of the presented model is illustrated in Fig. 2 by the graph of a typical force–displacement relationship plotted in the nanoscale, where the total path of the interaction in the forward direction of the loading is denoted by a solid curve

passing through the points S, L and U and through the points U, L and S in the backward direction. It is assumed that the particle's interaction with the plane surface occurs at the time instant t_S which is set as initial time t_0. At the time instance t_S the bacterium approaches the plane surface with the velocity υ_0. The starting point in Fig. 2 is denoted by S.

Beginning at the interaction distance $a_{F=0}$, up to zero (Fig. 2, curve S–L) the bacterium is attracted to the plane by a short range $F^N_{adh}(t)$ van der Waals adhesion force, $F^N_{dl}(t)$ electrostatic double layer force and steric force $F^N_{steric}(t)$ without any contact. During the approach, in time interval $(t_0 \leqslant t \leqslant t_L)$, the particle is attracted to the plane by this force.

$$F^N_{appr}(t) = F^N_{dl}(t) + F^N_{steric}(t) + F^N_{adh}(t) \tag{5}$$

The adhesive short-range van der Waals adhesion force is defined as suggested by Tomas [37,28]:

$$F^N_{adh}(t) = -\frac{\left|F^N_{L,adh}\right| a^2_{F=0}}{\left(a_{F=0} - h(t)\right)^2}, \tag{6}$$

where $F^N_{L,adh}$ is the adhesion (or the so-called jump in) force of a rigid contact without any contact deformation.

Here, displacement during approach $h < 0$ is negative. In Eq. (6) the decay of the van der Waals interaction between a bacterium and a plane is defined as inverse square of the bacterium-plane distance, while at the characteristic adhesion distance $a_{F=0}$ is assumed. Thus, analytically the description of the path of the adhesive contactless approach is relevant to two physical parameters – the characteristic influence of adhesion distance $a_{F=0}$ and the adhesion force $F^N_{L,adh}$ (the so-called jump-in force) defined at point zero of the considered diagram with zero displacement $h = 0$. The time dependent electrostatic double-layer force $F^N_{dl}(t)$ and steric force $F^N_{steric}(t)$ will be introduces below.

The approach continues until the particle reaches the surface at the time instant t_L with the negative displacement varying in the range up to zero distance $h(t_L) = 0$ denoted by point L on the graph. We assume that at this moment the bacterium is in contact with the interacting surface. At the moment when the bacterium and the surface start to get into contact it is described by force F^N_L. Theoretically the force F^N_L is a sum of attractive adhesion force $F^N_{L,adh}$ and repulsive electrostatic double-layer force $F^N_{L,dl}$, steric force $F^N_{L,steric}$ components:

$$F^N_L = F^N_{L,dl} + F^N_{L,steric} + F^N_{L,adh} \tag{7}$$

The contact of the bacterium with the surface begins with the formation of the adhesion force $F^N_{L,adh}$. The force $F^N_{L,adh}$ is related to the interfacial energy γ of the interacting bodies. In the case of the DMT model, see (Derjaguin et al. [38]), theoretically it is defined as:

$$F^N_{L,adh} = F_{DMT} = -4 \cdot \pi \cdot R_{eff} \cdot \gamma_A \tag{8}$$

here R_{eff} – effective radius of interacting particles, while γ_A – conventional surface energy standing for a physical constant.

When the approaching surface charges have the same sign, the concentration of ions between the surfaces always increases. This results in a repulsive electrostatic double layer force. The electrostatic double-layer repulsion force makes contact complicated and limits the ability of the bacterium to stick to a surface. The electrostatic double-layer force arises because of surface charges at the interfaces. Following continuum theory Butt et al. [20] present the potential distribution which is determined from the Poisson–Boltzmann model, which is a second order differential equation, to describe electrostatic interactions between molecules in ionic solutions. This repulsive electrostatic double-layer force $F^N_{dl}(t)$ is given as:

$$F^N_{dl}(t) = F^N_{L,dl} \cdot \mathrm{e}^{h(t)/\lambda_D} \tag{9}$$

The extended version of Eq. (9) can be found in Butt [39] and obtained results are similar to those by Hogg et al. [40], were potential energy between two surfaces with constant surface potential was calculated. In Eq. 9 $F^N_{L,dl}$ is the electrostatic double-layer force at a point L and distance $h = 0$, where the bacterium starts to contact with a surface. At this point L, the double-layer force is $F^N_{L,dl}$:

$$F^N_{L,dl} = 4\pi \cdot R_{eff} \varepsilon \varepsilon_0 \psi_i \psi_j \lambda_D^{-1}, \tag{10}$$

where ψ_i, ψ_j are surface potentials of bacteria i and a interacting surface j (in V), ε the dielectric constant of the medium, ε_0 the permittivity of free space with $\varepsilon_0 = 8.854 \cdot 10^{-12}$ C^2 J^{-1} m^{-1}, λ_D the Debye length (in nm). The electrostatic double-layer force decays roughly exponentially. The effective decay length is described as Debye length $\lambda_D = 0.304/\sqrt{c}$, where c is the concentration of the electrolyte in mol l^{-1}. In this work the value of the concentration of the electrolyte c is equal to the ionic strength M.

Bacteria cells have a surface that is studded with biological polymers and these polymer brushes can cause steric repulsion when they are confined to a narrow space (Linke and Goldman [41]). For the description of the steric force the modified Alexander-de Gennes model [42,43] is used, Butt et al. [44]:

$$F^N_{steric}(t) = 50 \cdot R_{eff} \cdot k_B \cdot T \cdot L_0 \cdot \Gamma^{3/2} \mathrm{e}^{2\pi \cdot h(t)/L_0} \tag{11}$$

Here k_B is the Boltzmann constant, T is the absolute temperature, Γ is the surface density of that same polymer on the cell surface or grafting density, L_0 is the equilibrium thickness of the polymer brush.

At the distance $h = 0$, at point L, the steric force is $F^N_{L,steric}$:

$$F^N_{L,steric} = 50 \cdot R_{eff} \cdot k_B \cdot T \cdot L_0 \cdot \Gamma^{3/2} \tag{12}$$

After particle reach point L, the loading process begins and follows the path of the loading between the points L and U. As a result, the loading stage is defined within the time interval $(t_L \leqslant t \leqslant t_U)$. It is characterized by a positive values of the contact displacement $h(t) > 0$. The contact force $F^N_{load,el}(t)$ of the loading comprising of the repulsive and attractive contributions is described as:

$$F^N_{load,el}(t) = F^N_{Hertz}(t) + F^N_{L,dl} + F^N_{L,steric} + F^N_{L,adh} \tag{13}$$

In this work we take into account adhesive elastic bacterium behaviour. For the spherical bacterium contact, the classical Hertz $F^N_{Hertz}(t)$ model is used and describes the bacterium-surface elastic contact:

$$F^N_{Hertz}(t) = \frac{2}{3} E_{eff} \sqrt{R_{eff} \cdot h(t)^3} \tag{14}$$

Here E_{eff} is the effective Young's modulus and R_{eff} is the effective radius. Both can be calculated as follows:

$$R_{eff} = \left(\frac{1}{R_i} + \frac{1}{R_j}\right)^{-1}; \quad E_{eff} = 2\left(\frac{1-\nu_i^2}{E_i} + \frac{1-\nu_j^2}{E_j}\right)^{-1} \tag{15}$$

Here R_i is the radius of the bacterium. R_j is the radius of the interacting target, which for a flat surface is $R_j = \infty$. The end of the loading phase is characterized by the maximal displacement of the contact point $h_U(t_U)$ reached at the time instant t_U. The unloading and detachment of a bacterium is described by applying developed

attractive–dissipative mechanisms, which will be introduced in the next attractive–dissipative model section.

3.3.1. Attractive–dissipative model

The dissipation of energy is a phenomenon significantly affecting the behaviour of particle systems. A major motivation for our work is associated with the study of a specific type of dissipation, the so-called "adhesion hysteresis", when the amount of energy required to separate two surfaces is greater than the amount of energy gained by bringing the surfaces together. This hysteresis behaviour of fine objects is a typical result observed in atomic force measurements (AFM), while the background of this process is still not fully understood. We take into account the change of the adhesion force during the unloading process because of the non-smooth surface of a bacterium. The hysteresis of normal interaction can be explained due to the inelastic deformation of the rough bacterium surface and a resulting increase of the adhesion force, which during deformation is presented as a time dependent function. It is known for microparticles that the adhesion force depends on the surface roughness, Rumpf [45], Schubert [46], Tomas [47]. Based on AFM experiments with bacteria by e.g. Ubbink and Schär-Zammaretti [19], Touhami et al. [26] and Abu-Lail et al. [27] it is known that the force–displacement curve has a hysteresis and shows a dissipative behaviour. Because of the change of surface roughness during deformation we take into account the increase of the attractive force during the unloading and detachment process. Because of the increase of the van der Waals force we additionally take into account the dissipative behaviour of the bacterium.

Empirically, it has been observed that the amount of energy W^N_{diss}, dissipated during a complete full approach-separation loop is characterized by the area between the approach-loading and unloading-detachment branches of the hysteretic force–displacement diagram of collision. In our case for adhesive elastic contact whole amount of dissipated energy W^N_{diss} during interaction is equal to dissipated energy due to attraction $W^N_{diss} = W^N_{attr,diss}$. The dissipated energy due to attraction $W^N_{attr,diss}$ can be related to the critical velocity, $\upsilon^N_{0,cr}$, of normal adhesive elastic interaction measured in physical experiments. If critical velocity $\upsilon^N_{0,cr}$ is known, as a result, the dissipated energy can be calculated as kinetic energy generated by the initial critical velocity:

$$W^N_{attr,diss} = \frac{m_{eff} \cdot \upsilon^{N2}_{0,cr}}{2}, \tag{16}$$

where m_{eff} is the effective mass of the interacting particles.

Eq. (16) presumes that, actually, adhesion or cohesion causes the sticking of the particles, and the dissipated energy, $W^N_{attr,diss}$, as well as the critical initial velocity, $\upsilon^N_{0,cr}$, determines the threshold of the behaviour of a bacterium during its sticking or rebound. A bacterium does not stick if the amount of the initial kinetic energy is higher than the amount of the critical energy dissipated due to the interaction. If the initial normal velocity, υ^N_0, is lower than the critical velocity $\upsilon^N_{0,cr}$ after an impact, the bacterium remains in the attractive zone and sticks to the interacting surface. Otherwise, if the value of the initial particle velocity is higher than the critical velocity $\upsilon^N_{0,cr}$, the bacterium leaves the surface. It is obvious that the critical velocity $\upsilon^N_{0,cr}$, or the dissipated energy $W^N_{attr,diss}$ defined by Eq. (16) can be regarded as the constants of interacting bodies that do not depend on the value of the impact velocity.

On the other hand, the dissipated energy can be calculated theoretically; the amount of dissipated energy due to adhesion during deformation may be presented as a product of two physical constants $F^N_{L,adh}$ and $a_{F=0}$, which were described earlier [29]. We take into account a comparable amount of known adhesion related energy dissipation in order to describe the energy dissipation during the deformation of the bacterium surface asperities. This product describes the adhesion work which is needed to detach the particle from the surface. With this dissipated energy related work we take into account the increase and change of influence of adhesion due to deformation of asperities. The dependence of the adhesion forces on surface roughness is a known phenomenon (comp. Tomas [37,47]). In this work, the theoretical amount of dissipated energy related to adhesion is calculated by the following equation:

$$W^N_{attr,diss} = h_{asperity}\left|F^N_{L,adh}\right| \tag{17}$$

Here the amount of dissipated energy due to adhesion during deformation may be presented as a product of two parameters, the adhesion force $F^N_{L,adh}$ and initial height of asperity $h_{asperity}$ on the bacterium surface. Dissipation energy $W^N_{attr,diss}$ is generated due to the change of the influence of adhesion because of the change of asperities during deformation. Because of the deformation, the influence of adhesion the force during rebound is different.

It should be noted that the variation of the dissipative force in the contact area due to the adhesion hysteresis has not been thoroughly investigated and the methodology for evaluation of this variation has not been developed yet. Some limited contributions could be mentioned. Feng et al. [48] have illustrated the phenomenon of the adhesion hysteresis in the JKR model by FEM simulations. Along with the JKR model, Severson et al. [49] have also considered the adhesion hysteresis by simulating the dynamics of a particle, while the dissipative contribution was characterized by a sudden jump of the normal force at the beginning of the unloading phase. Sahagún and Sáenz [50] simulated the adhesive hysteresis and presented a model for the unilateral distribution of dissipative forces.

To capture the dissipated energy in an adhesion hysteresis, we introduce the attractive–dissipative force $F^N_{attr,diss}(t)$, which acts during the rebound motion within the entire displacement interval between the maximal displacement h_U and the separation, $a_{F=0}$. This path is denoted on the graph in Fig. 2 by points U, A and D. To grasp the variation of this force during unloading, the additional weighting function,

$$\bar{h}(t) = (h_U - h(t))/(h_U - h_A) \tag{18}$$

is introduced, where h_U is the maximum normal displacement of the interacting bodies and $\bar{h}(t)$ is the relevant displacement of the bacterium. This function linearly increases from zero at the point U up to 1 at the point A. During detachment $\bar{h}(t) = 1$. For the adhesive elastic contact displacement $h_A = 0$. Consequently, the suggested variation implies that the maximum value of the dissipation force $F^N_{A,adh,diss}$ is reached at the detachment point A, with the zero displacement $h = 0$. Finally, we relate this value to the amount of dissipated energy:

$$F^N_{A,adh,diss} = -\frac{2 \cdot W^N_{attr,diss}}{a_{F=0} + h_U - h_A} \tag{19}$$

In this paper the amount of dissipated energy $W^N_{attr,diss}$ is related to the change of the influence of attraction and it is fixed and independent of the initial velocity as outlined by Jasevičius et al. [29].

Generally, the time dependent adhesive dissipative force $F^N_{adh,diss}(t)$ is given as:

$$F^N_{adh,diss}(t) = F^N_{A,adh,diss} \cdot \bar{h}(t), \tag{20}$$

here the normalized displacement $\bar{h}(t)$ is needed to achieve the final energy balance during interaction during unloading and detachment. During the unloading in the time interval ($t_U \leqslant t \leqslant t_A$), the contact force follows the reversed loading path between the points U and L (Fig. 2). Consequently, the unloading force $F^N_{unload,el}(t)$ may be described as:

$$F^N_{unload,el}(t) = F^N_{Hertz}(t) + F^N_{L,dl} + F^N_{L,steric} + F^N_{L,adh} + F^N_{adh,diss}(t) \tag{21}$$

During unloading, when the bacterium reaches point A, the bacterium normal force and its attractive–dissipative force are equal:

$$F^N_A = F^N_{L,dl} + F^N_{L,steric} + F^N_{L,adh} + F^N_{A,adh,diss} \tag{22}$$

After reaching point A, the detachment process begins. The detachment describing force $F^N_{detach,el}(t)$ follows the reversed path of the approach between the points A and D. For the bacterium this force has a repulsive and the van der Waals force related attractive–dissipative behaviour. The detachment force $F^N_{detach,el}(t)$ is acting within the time interval, ($t_A \leqslant t \leqslant t_D$) and is given by:

$$F^N_{detach,el}(t) = F^N_{dl}(t) + F^N_{steric}(t) + F^N_{A,adh}(t) \tag{23}$$

Here, the load dependent adhesion force during detachment is described:

$$F^N_{A,adh}(t) = -\frac{\left(\left|F^N_{L,adh}\right| + \left|F^N_{A,adh,diss}\right|\right) \cdot a^2_{F=0}}{\left(a_{F=0} - h(t)\right)^2} \tag{24}$$

It is important to mention here, that displacement $h(t)$ during detachment is negative $h < 0$. The interaction is assumed to be terminated at the point D at the final time instant t_D.

3.4. Adhesive elastic–plastic contact

The constitutive model for the normal contact, combining elastic–plastic contact deformation behaviour and including adhesion, is shown in Fig. 3. Generally, the particle behaves in the same manner as described in the case of an elastic contact. The constitutive interaction model may be illustrated by the diagram (S–L–Y–U–A–D) of force $F^N \equiv F^N_i$ and displacement h plotted in Fig. 3. Here we present a theoretical model for defining the normal interaction involving two parts. A negative displacement occurs when the left part covers the bacterium approach (S–L) and the detachment (A–D). A positive displacement takes place when the right part includes the elastic loading (L–Y) and the elastic–plastic loading (Y–U), while the unloading is elastic (U–A). The elasticity limit is indicated by the yield point Y. At the adhesion limit at point A, finally, the bacterium detaches with increasing separation, line A–D. The displacement at approach (S–L) and detachment (A–D) corresponds to the interaction with no contact and no deformation, whereas the displacement at (L–Y–U–A) coincides with the interaction with contact when the bacterium deforms. Negative normal force agrees with attraction while positive – with repulsion. The elastic–plastic deformation here is based on the model by Tomas, see Tomas [28].

The particle movement starts at the minimal initial distance $a_{F=0}$ by approaching the plane at the initial velocity υ_0. It could be stated that the adhesion force $F^N_{appr}(t)$, acting on the particle below distance $a_{F=0}$ is defined by Eq. (5). When the particle reaches the surface, the Hertz contact is elastic, and the normal force during loading is defined by Eq. (13). With increasing external normal load, the soft contact reaches the elastic–plastic limit under pressure p_f. Here this deformation limit is presented with displacement h_Y and contact radius r_Y when it reaches the point Y:

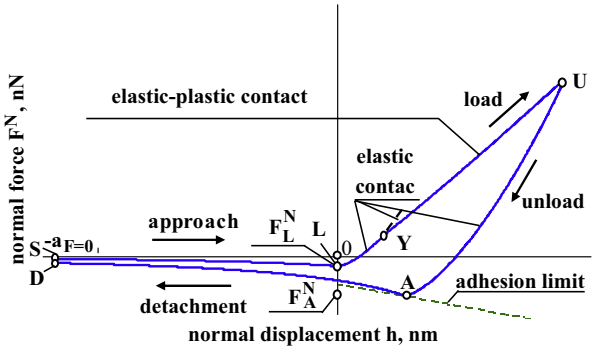

Fig. 3. Model for the adhesive elastic–plastic interaction of a cell. Force displacement relations are given for an elastic–plastic contact. The normal force–displacement diagram of the characteristic contact flattening of the bacterium is modelled by that of an ultrafine particle. The bacterium approaches, line S–L, Eq. (5), forms an elastic contact, line L–Y, Eq. (13), starts with yielding at point Y and forms an elastic–plastic contact, line Y–U, Eq. (26), can be unloaded at point U, line U–A, Eq. (30), achieves the adhesion limit at point A, and finally, detaches with increasing separation, line A–D, Eq. (34). The necessary material data for this diagram are characteristic parameters of adhesions such as minimum centre separation $a_{F=0}$ and adhesion force of a rigid contact without any contact deformation $F^N_{L,adh}$, electrostatic double-layer force F^N_{dl}, steric force F^N_{steric} and elasticity parameters such as modulus of elasticity E and Poisson ratio ν, plasticity parameters such as micro-yield strength of the bacterium p_f, elastic–plastic contact area coefficient κ_A and plastic repulsion coefficient κ_p, are given in the Basic data of the simulation section.

$$h_Y = \frac{r^2_Y}{R_{eff}} \tag{25}$$

Thereafter the nonlinear elastic–plastic contact force is described as follows:

$$F^N_{load,el-pl}(t) = F^N_{el-pl}(t) + F^N_{L,dl} + F^N_{L,steric} + F^N_{L,adh} \tag{26}$$

Elastic–plastic force $F^N_{el-pl}(t)$ is described basing on Tomas model [28]:

$$F^N_{el-pl}(t) = \pi \cdot R_{eff} \cdot p_f \cdot \left(\kappa_A - \kappa_p\right) \cdot h(t) \tag{27}$$

Here, κ_A is the dimensionless elastic–plastic contact area coefficient which is representing the ratio of plastic particle contact deformation to the total contact deformation area, while κ_p is the dimensionless plastic repulsion coefficient and p_f is the micro-yield strength of the bacterium. These coefficients are described in [28]. During the contact of the bacterium and the interacting surface, the electrostatic double-layer force and steric force are assumed to be time independent and presented as $F^N_{L,dl}$ and $F^N_{L,steric}$. The point Y is reached when the displacement h_Y is reached which can be described by the formula (Tomas [28]):

$$h_Y = R_{eff} \cdot \left[\frac{3 \cdot \pi \cdot p_f \cdot \left(\kappa_A - \kappa_p\right)}{4 \cdot E_{eff}}\right]^2 \tag{28}$$

The elastic–plastic repulsion force is obtained by integrating the cutoff shaped contact pressure profile. The integration results may be evaluated by introducing the dimensionless elastic–plastic contact area coefficient κ_A, representing the ratio of plastic particle contact deformation area A_{pl} to total contact deformation area $A_{area} = A_{pl} + A_{el}$, and expressed in terms of the displacement as:

$$\kappa_A = 1 - \frac{1}{3}\sqrt[3]{\frac{h_Y}{h(t)}} \tag{29}$$

The yield displacement reflects the propagation of yielding. The lower limit $\kappa_A = 2/3$ corresponds to the solely elastic contact deformation $A_{pl} = 0$. The upper bound $\kappa_A = 1$ indicates the complete

yielding of the contact ($A_{pl} = A_{area}$). For simplification of the final expression, a dimensionless coefficient κ_p, referred to here as a plastic repulsion coefficient, was introduced. For rigid (ideally hard) contacts, this plastic repulsion coefficient is infinitely small, i.e. $\kappa_p \approx 0$, while for soft or compliant contact $\kappa_p \to 1$.

When the bacterium reaches the maximal overlap h_U, the contact is elastically unloaded at point U until the deformation path reaches the adhesion limit at point A. During unloading the prescribed time dependent adhesive dissipative force $F^N_{adh,diss}(t)$ is described in the similar way as described for the elastic one. The resultant force during the unloading may be expressed as follows:

$$F^N_{unload,el-pl}(t) = F^N_{A,Hertz}(t) + F^N_{L,dl} + F^N_{L,steric} + F^N_{L,adh} + F^N_{adh,diss}(t) - \Delta F^N(h_U), \tag{30}$$

for the contact unload between h_U and h_A. Here elastic unloading is described basing on elastic Hertz force:

$$F^N_{A,Hertz}(t) = \frac{2}{3} \cdot \frac{E}{1-\nu^2} \cdot \sqrt{R_{eff}} \cdot (h(t) - h_A)^{3/2} \tag{31}$$

During unloading, when bacterium reaches point A, normal force is:

$$F^N_A = F^N_{L,dl} + F^N_{L,steric} + F^N_{L,adh} + F^N_{A,adh,diss} - \Delta F^N(h_U), \tag{32}$$

here, $\Delta F^N(h_U)$ presents a residual force, reflecting the elastic–plastic deformation history. The detachment process begins, when a bacterium reaches the adhesion limit at point A during unloading. The adhesion limit may be expressed as follows:

$$F^N_{adh,limit}(h_A) = F^N_{L,dl} + F^N_{L,steric} + F^N_{L,adh} + F^N_{A,adh,diss} - \pi R_{eff} p_{vdW} h_A, \tag{33}$$

here p_{vdW} is the attractive van der Waals pressure [28] used to describe the adhesive interaction and can be calculated as $p_{vdW} = \kappa_p p_f$.

The detachment of the bacterium between displacements h_A and $a_{F=0}$ (points A–D) is described as follows:

$$F^N_{detach,el-pl}(t) = F^N_{A,dl}(t) + F^N_{A,steric}(t) + F^N_{A,adh}(t), \tag{34}$$

During detachment, load dependent adhesion force $F^N_{A,adh}(t)$ is:

$$F^N_{A,adh}(t) = -\frac{\left(\left|F^N_{L,adh}\right| + \left|F_{A,adh,diss}\right|\right) \cdot a^2_{F=0}}{(a_{F=0} + h_A - h(t))^2} - \frac{\pi \cdot R_{eff} \cdot p_{vdW} \cdot h_A}{(a_{F=0} + h_A - h(t))^3} \cdot a^3_{F=0} \tag{35}$$

During detachment, for the adhesive elastic–plastic contact, the double-layer electrostatic force and steric force are described below, by modifying the Poisson–Boltzmann model and Alexander-de Gennes model by adding the displacement h_A. The double-layer electrostatic force $F^N_{A,dl}(t)$ during detachment is given as:

$$F^N_{A,dl}(t) = F^N_{L,dl} \cdot e^{-(h_A - h(t))/\lambda_D} \tag{36}$$

The steric force $F^N_{A,steric}(t)$ during detachment is given as:

$$F^N_{A,steric}(t) = F^N_{L,steric} \cdot e^{-2\cdot\pi(h_A - h(t))/L_0} \tag{37}$$

During the elastic–plastic interaction as in the elastic case, interaction is assumed to be terminated at the point D at the final time instant t_D.

4. Basic data of simulation

In this work the interaction of a spherical cell with a flat surface is investigated which involves the *S. aureus* bacterium interaction with a glass surface using an attractive–dissipative model. Detailed description of the attractive–dissipative model is given in Jasevičius et al. [29,30]. Basic data on the parameters of *S. aureus* and the glass surface are taken from Reeks et al. [51], Ibrahim et al. [52] and Linke and Goldman [41]. A bacterium can travel in the air in a bioaerosol, while the velocity of bioaerosol droplets can reach values of up to 4 m/s (Paez-Rubio et al. [53]). The behaviour of the whole bioaerosol droplet during the impact here is not analysed. The presented investigation is limited to the interaction of a bacterium and a target surface within a liquid medium. The initial impact velocity of the bacterium on the target surface is equal to the impact velocity of the bioaerosol droplet and set to 0.1 m/s. Initially, the *S. aureus* bacterium has a distance of $a_{F=0} = 20$ nm from the glass surface. The diameter of the bacterium is $d = 1$ μm, while the density is $\rho_i = 1.415$ g/cm^3 following Bakken and Olsen [54]. The density of the glass surface is $\rho_j = 2.470$ g/cm^3. The elastic modulus of native *S. aureus* is 1.33 ± 0.21 MPa as stated by Jin et al. [55] and set to $E_i = 0.0012$ GPa. Poisson's coefficients for living cells can vary from 0.3 to 0.5 (Butt et al. [20]) and are set to $\nu_i = 0.5$ as proposed by Touhami et al. [56]. The elastic modulus of glass is considered with $E_j = 80.1$ GPa, the Poisson's coefficient is $\nu_j = 0.27$. The interaction of the bacterium and the glass surface is investigated within a liquid medium. For the interaction in water (pH 7), the ionic strength is taken as ~0.1 M following Linke and Goldman [41]. The surface potentials of the glass surface and *S. aureus* are, respectively, –35 mV and –6 mV as given by Ducker et al. [57], Prince and Dickinson [58] and Linke and Goldman [41]. For the investigation of the bacterium and the surface interaction the Debye length value is chosen as $\lambda_D = 10$ nm. The Boltzmann's constant is $k_B = 1.381 \cdot 10^{-23}$ J K^{-1}. The dielectric constant of water is $\varepsilon = 78.54$ at a temperature T of 298 K; the permittivity of free space is $\varepsilon_0 = 8.854 \cdot 10^{-12}$ C^2 J^{-1} m^{-1}. The valence of electrolyte ions $z = 1$ for NaCl and the charge of an electron is $e_c = 1.602 \cdot 10^{-19}$ C. The initial adhesion force is set to $F^N_{L,adh} = -0.25$ nN, see Jin et al. [55] and Touhami et al. [26]. With these values the theoretical forces between the *S. aureus* bacterium and the glass surface were calculated. In order to describe the elastic–plastic behaviour of the bacterium there are no parameters of micro-yield strength of a bacterium known from literature. Therefore it is freely chosen as a small value and set to $p_f = 100$ kPa which leads to a yield limit of $h_Y = 2.89$ nm. The dimensionless plastic repulsion coefficient needed for the calculation is set to $\kappa_p = 0.15$. The *S. aureus* asperity height $h_{asperity}$ can vary from 1.6 ± 0.3 nm to 5.4 ± 1.2 nm (Francius et al. [13]). Here an asperity height $h_{asperity} = 2$ nm was taken into account. Equilibrium thickness of the polymer brush L_0 is 90 nm (Yongsunthon and Lower [59]) and the grafting density Γ is set to $3.4 \cdot 10^{14}$ m^{-2}, see Linke and Goldman [41].

5. Results

The numerical results obtained describe the theoretical *S. aureus* behaviour during the interaction with a glass surface. The bacterium is interpreted as an active colloid particle which has the ability to be attracted to a surface by adhesion forces. The results show the different behaviour of the bacterium interaction using two models for elastic and elastic–plastic deformation. The models are based on the DMT, DLVO and Tomas models. The two deformation models are typical for non-biological particles, while they can be also applied for bacteria. Under the applied idealizations and the implementation of the interaction model for the description of the deformation process the theoretical behaviour of a bacterium becomes similar to the behaviour of a deformed colloid particle. The bacterium is described by two different adhesive elastic and adhesive elastic–plastic interaction models by applying previously

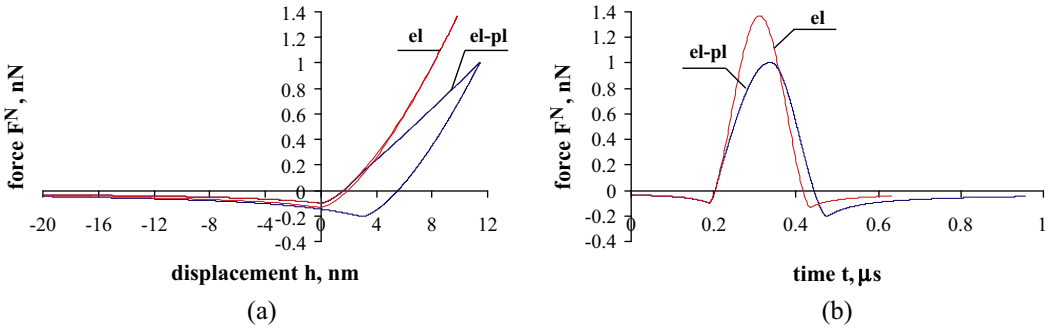

Fig. 4. Results of the bacterium interaction with a flat surface (a) – normal force F^N versus displacement h, (b) – normal force F^N time history.

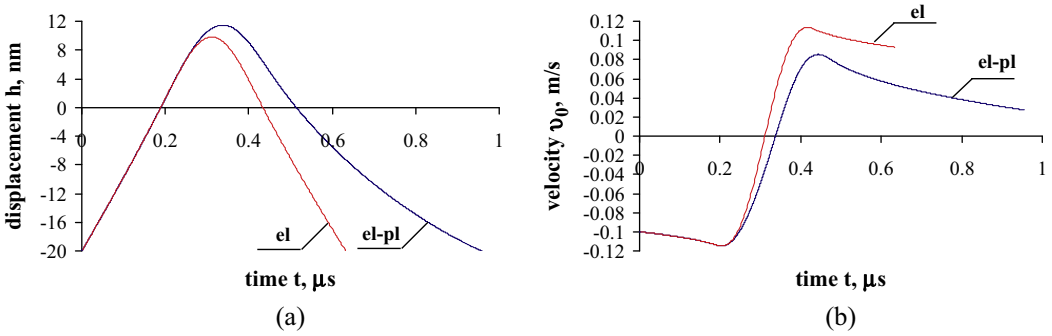

Fig. 5. Results of a bacterium interaction with a flat surface (a) – displacement h history, (b) – velocity υ history.

developed energy dissipation mechanisms related to adhesion. This condition allows us to investigate the varying influences of electrostatic forces as well as van der Waals forces during the bacterium interaction and deformation. The time dependent electrostatic double-layer force is described using a Poisson–Boltzmann based model [39]. During deformation, it is assumed that in the first case elastic deformation is described with the time dependent Hertz model, while for the second case elastic–plastic material behaviour is described basing on the Tomas model. The adhesive elastic model includes energy dissipation mechanism related to the influence of adhesion, while the adhesive elastic–plastic model additionally includes energy dissipation mechanisms related to elastic–plastic contact. Two energy dissipation mechanisms make the adhesive elastic and elastic–plastic interaction models more complicated and respectively change the behaviour of the bacterium during interaction. The differences of the two kinds of interactions can be observed in the following results.

The bacterium interaction with elastic deformation is presented in Figs. 4 and 5 with a red[1] line, elastic–plastic with a blue line. Interaction, when interacting surfaces are at distance, is described with time dependent attractive van der Waals and repulsive electrostatic double-layer, steric forces. The comparisons of two different interactions show the influence of the elastic–plastic deformation on the bacterium during the interaction process. The presented results in Figs. 4 and 5 show the hysteresis behaviour of the bacterium. The amount of dissipated energy during elastic interaction is equal to the energy dissipation related to attraction $W^N_{diss} = W^N_{attr,diss}$. This amount of energy dissipation $W^N_{attr,diss}$ is independent of the initial velocity, Jasevičius et al. [29] and equal to $W^N_{attr,diss} = h_{asperity}\left|F^N_{L,adh}\right| = 5 \cdot 10^{-19}$ J. This amount of energy is important to take into account for the hysteresis behaviour of the bacterium dissipative interaction and for the description of the sticking process as well as to gain the initial critical sticking velocity $\upsilon_{0,cr}$, which is $\upsilon_{0,cr,el} = -0.03674$ m/s in the presented model with elastic deformation. During adhesive elastic–plastic interaction additional dissipation is achieved by elastic–plastic dissipation $W^N_{diss} = W^N_{diss,attr} + W^N_{diss,el-pl}$, while the value of the amount of dissipated energy related to attraction $W^N_{attr,diss}$ is the same for both models. The larger the amount of dissipated energy W^N_{diss} during adhesive elastic–plastic contact the higher the value of critical velocity which is equal to $\upsilon_{0,cr,el-pl} = -0.08961$ m/s for the investigated adhesive elastic–plastic case.

A force displacement diagram is shown in Fig. 4a, while the time history of the normal force is presented in Fig. 4b. The first diagram 4a shows the hysteresis behaviour of the bacterium. These Fig. 4a and b show that the dissipation related to adhesion and elastic–plastic deformation influences the bacterium. Here negative force means attraction, while positive means repulsion. Generally, positive displacement means interaction with contact deformation, while negative displacement means interaction without any contact deformation.

Basing on the DLVO model for the description of the interaction at a distance, the positive values of the normal force can be reached and the overall behaviour can be of repulsive manner. Results show, that during approach and detachment ($h < 0$) the repulsive steric and electrostatic double-layer forces become not dominant for a bacterium moving in a liquid medium and in both cases of the models the approach and detachment remains to be governed by negative forces and attractive manner. Attractive manner is typical for interacting ultrafine objects at a distance, otherwise the approach behaviour depends on the surrounding media. The attraction force is negative, otherwise in Fig. 4a and b it was observed, that because of the action of the repulsive electrostatic double-layer and steric forces, the influence of the attractive van

[1] Colorful Figures are presented in web version of article.

der Waals force decreases. At a displacement $h_L = 0$ the normal force value is $F_L^N = -0.1002$ nN, which is divided in the contribution of the adhesion force $F_{L,adh}^N = -0.25$ nN and double-layer force $F_{L,dl}^N = 0.09175$ nN, $F_{L,steric}^N = 0.05805$ nN, $F_L^N = F_{L,dl}^N + F_{L,steric}^N + F_{L,adh}^N$.

At a displacement of $h_A = 2.9917$ nm the normal force can be calculated as $F_A^N = F_{A,dl}^N + F_{A,steric}^N + F_{A,adh}^N$ and for elastic contact it is $F_A^N = -0.1337$ nN, while for elastic plastic contact $F_A^N = -0.2058$ nN. The double-layer and steric force values are the same as at point L, $F_{A,dl}^N = F_{L,dl}^N$, $F_{A,steric}^N = F_{L,steric}^N$, for an adhesive elastic contact and an adhesive elastic–plastic contact. Adhesion force for elastic contact is $F_{A,adh}^N = -0.2835$ nN, while for elastic–plastic contact it is $F_{A,adh}^N = -0.3556$ nN.

During deformation different models result in a different behaviour of the bacterium. Using the adhesive elastic contact (red line) higher values of the normal force than for adhesive elastic–plastic contact (blue line) are observed. Also using an elastic–plastic model, the bacterium becomes more deformed during loading – this is shown by higher displacement values (Figs. 4 and 5a). In both deformation cases, during unloading and detachment the normal force is lower. In the presented models it is assumed that an increase of the attractive forces results out of the influence of the surface roughness, see Jasevičius et al. [29–32]. The dissipation is stronger at elastic–plastic contact, rebound velocity for the elastic interaction is $\upsilon_{r,el} = 0.09301$ m/s and for the elastic–plastic interaction $\upsilon_{r,el-pl} = 0.02713$ m/s (Fig. 5b). The amount of adhesion related dissipated energy is fixed and independent of the initial interaction velocity. As the elastic–plastic model gives additional dissipation to the bacterium interaction, the duration of the interaction of the bacterium with the elastic–plastic contact becomes longer.

Further research is necessary to apply the numerical investigations of the sticking behaviour of bacteria to the formation of biofilms, Šimkus et al. [60], which could be achieved by applying theoretical viscous damping models used for ultrafine particles, (Jasevičius et al. [61]), as well as oblique interaction, Jasevičius et al. [30,35].

6. Conclusion

The adhesive elastic dissipative and adhesive elastic–plastic dissipative models were introduced for bacteria plane surface interaction within a liquid medium. The primary interest of this paper was given to bacterium behaviour by applying the presented adhesive elastic–plastic model. The implementation of an elastic Hertz and elastic–plastic Tomas model for the description of the deformation process, results in a theoretical behaviour of a bacterium similar to that of a deformed body. The implemented energy dissipation mechanism related to adhesion agrees with known DLVO, DMT, Hertz and Tomas models. In the presented approach with two different adhesive elastic and adhesive elastic–plastic models the amount of dissipated energy was the same and it is independent of the initial velocity and the type of the model. This behaviour is typical for non-biological particles, while it can be also applied to the simulation of bacteria interaction. This condition is useful for the description and simulation of bacteria motion as well as for the creation of structures such as biofilms. Results show that with the adhesive elastic–plastic model, the bacterium becomes more deformed. In both elastic and elastic–plastic deformation cases, during unloading and detachment the normal force is lower. This is because in the presented models it was assumed that attractive forces increase because of the change of the surface roughness during deformation. The implementation of the influence of adhesive and electrostatic double-layer forces was needed for the description of the interaction of the bacterium at a distance of the surface. By applying a repulsive electrostatic double-layer force and steric force models, during the bacterium approach process, positive values of the normal force were not reached and the overall behaviour was of dominant attractive manner. Finally, the attractive manner during interaction at a distance can be observed for different natural ultrafine objects, both non-biological as well as biological such as bacteria.

Acknowledgments

Raimondas Jasevičius is a postdoc at the Vilnius University. Postdoctoral fellowship is being funded by European Union Structural Funds project "Postdoctoral Fellowship Implementation in Lithuania".

Harald Kruggel-Emden is funded by German Research Foundation DFG through Grant No. KR3446/6-1.

References

[1] J.W. Tang, Y. Li, I. Eames, P.K.S. Chan, G.L. Ridgway, Factors involved in the aerosol transmission of infection and control of ventilation in healthcare premises, J. Hosp. Infect. 64 (2006) 100–114.
[2] M.C. Todd, M.V.F. Belteton, Factors involved in aerosol transmission of infection and control of ventilation in healthcare, Noninvas. Ventilation High-Risk Infect. Mass Casualty Events (2014) 269–277.
[3] B. Derjaguin, L. Landau, Acta Phys. Chem. URSS 14 (1941) 633.
[4] E.J.W. Verwey, J.Th.G. Overbeek, Theory of the stability of lyophobic colloids, J. Phys. Chem. 51 (1947) 631–636.
[5] V.M. Muller, V.S. Yushchenko, B.V. Derjaguin, General theoretical consideration of the influence of surface forces on contact deformations and the reciprocal adhesion of elastic spherical particles, J. Colloid Interface Sci. 92 (1983) 92–101.
[6] I.U. Vakarelski, A. Toritani, M. Nakayama, K. Higashitani, Effects of particle deformability on interaction between surfaces in solutions, Langmuir 19 (2003) 110–117.
[7] M. Hermanssom, The DLVO theory in microbial adhesion, Colloids Surf. B: Biointerfaces 14 (1999) 105–119.
[8] J. Azeredo, J. Visser, R. Oliveira, Exopolymers in bacterial adhesion: interpretation in terms of DLVO and XDLVO theories, Colloids Surf. B: Biointerfaces 14 (1999) 141–148.
[9] Y.H. An, R.J. Friedman, Concise review of mechanisms of bacterial adhesion to biomaterial surfaces, J. Biomed. Mater. Res. 43 (1988) 338–348.
[10] M. Ulrich, S. Herbert, J. Berger, G. Bellon, D. Louis, G. Münker, G. Döring, Localization of *Staphylococcus aureus* in infected airways of patients with cystic fibrosis and in a cell culture model of *S. aureus* adherence, Am. J. Respir. Cell Mol. Biol. 19 (1998) 83–91.
[11] L. Zhao, D. Schaefer, M.R. Marten, Assessment of elasticity and topography of *Aspergillus nidulans* spores via atomic force microscopy, Appl. Environ. Microbiol. 71 (2005) 955–960.
[12] L.G. Harris, R.G. Richards, *Staphylococcus aureus* adhesion to different treated titanium surfaces, J. Mater. Sci.: Mater. Med. 15 (2004) 311–314.
[13] G. Francius, O. Domenech, M.P. Mingeot-Leclercq, Y.F. Dufrene, Direct observation of *Staphylococcus aureus* cell wall digestion by lysostaphin, J. Bacteriol. 190 (2008) 7904–7909.
[14] N. Mitik-Dineva, J. Wang, V.K. Truong, P. Stoddart, F. Malherbe, R.J. Crawford, E.P. Ivanova, *Escherichia coli*, *Pseudomonas aeruginosa*, and *Staphylococcus aureus* attachment patterns on glass surfaces with nanoscale roughness, Curr. Microbiol. 58 (2009) 268–273.
[15] S.E. Cramton, C. Gerke, N.F. Schnell, W.W. Nichols, F. Götz, The intercellular adhesion (ica) locus is present in *Staphylococcus aureus* and is required for biofilm formation, Infect. Immun. 67 (1999) 5427–5433.
[16] D. Mack, P. Becker, I. Chatterjee, S. Dobinsky, J.K.-M. Knobloch, G. Peters, H. Rohde, M. Herrmann, Mechanisms of biofilm formation in *Staphylococcus epidermidis* and *Staphylococcus aureus*: functional molecules, regulatory circuits, and adaptive responses, Int. J. Med. Microbiol. 294 (2004) 203–212.
[17] K.Y. Ha, Y.G. Chung, S.J. Ryoo, Adherence and biofilm formation of *Staphylococcus epidermidis* and *Mycobacterium tuberculosis* on various spinal implants, Spine 30 (2005) 38–43.
[18] A.T. Poortinga, R. Bos, W. Norde, H.J. Busscher, Electric double layer interactions in bacterial adhesion to surfaces, Surf. Sci. Rep. 47 (2002) 1–32.
[19] J. Ubbink, P. Schär-Zammaretti, Colloidal properties and specific interactions of bacterial surfaces, Curr. Opin. Colloid Interface Sci. 12 (2007) 263–270.
[20] H.-J. Butt, B. Cappella, M. Kappl, Force measurements with the atomic force microscope: technique, interpretation and applications, Surf. Sci. Rep. 59 (2005) 1–152.
[21] F. Gaboriaud, Y.F. Dufrêne, Atomic force microscopy of microbial cells: application to nanomechanical properties, surface forces and molecular recognition forces, Colloids Surf. B: Biointerfaces 54 (2007) 10–19.

[22] N.I. Abu-Lail, T.A. Camesano, The effect of solvent polarity on the molecular surface properties and adhesion of *Escherichia* coli, Colloids Surf. B: Biointerfaces 51 (2006) 62–70.
[23] V. Lulevich, T. Zink, H.Y. Chen, F.T. Liu, G.Y. Liu, Cell mechanics using atomic force microscopy-based single-cell compression, Langmuir 22 (2006) 8151–8155.
[24] L. Sirghi, Atomic force microscopy indentation of living cells. In: A. Méndez-Vilas, J. Díaz (Eds.), Microscopy: Science, Technology. Applications and Education, 2010, pp. 433–440.
[25] A. Méndez-Vilas, A.M. Gallardo-Moreno, R. Calzado-Montero, M.L. González-Martín, AFM probing in aqueous environment of *Staphylococcus epidermidiscells* naturally immobilised on glass: Physico-chemistry behind the successful immobilisation, Colloids Surf. B: Biointerfaces 63 (2008) 101–109.
[26] A. Touhami, M.H. Jericho, T.J. Beveridge, Atomic force microscopy of cell growth and division in *Staphylococcus aureus*, J. Bacteriol. 186 (2004) 3286–3295.
[27] L. Abu-Lail, Y. Tao, P.A. Pinzón-Arango, A. Howell, T.A. Camesano, Using atomic force microscopy to measure anti-adhesion effects on uropathogenic bacteria, observed in urine after cranberry juice consumption, J. Biom. Nanobiotech. 3 (2012) 533–540.
[28] J. Tomas, Adhesion of ultrafine particles – a micromechanical approach, Chem. Eng. Sci. 62 (2007) 1997–2010.
[29] R. Jasevičius, J. Tomas, R. Kačianauskas, Simulation of normal impact of ultrafine silica particle on substrate, Particul. Sci. Tech. 29 (2011) 107–126.
[30] R. Jasevičius, J. Tomas, R. Kačianauskas, D. Zabulionis, Simulation of adhesive dissipative behaviour of a microparticle under the oblique impact, Particul. Sci. and Tech. 32 (2014) 486–497.
[31] R. Jasevičius, R. Baronas, R. Kačianauskas, R. Šimkus, Numerical modeling of bacterium-surface interaction by applying DEM, Procedia Eng. Elsevier 102 (2015) 1408–1414.
[32] R. Jasevičius, R. Baronas, R. Kačianauskas, H. Kruggel-Emden, Modelling of the normal elastic dissipative interaction of a *S. aureus* bacterium, AIP Conference Proceedings of ICNAAM, vol. 1648, 2015, p. 400005.
[33] H. Kruggel-Emden, F. Elskamp, Modeling of screening processes involving non-spherical particles with the discrete element method, Chem. Eng. Tech. 37 (2014) 847–856.
[34] H. Kruggel-Emden, T. Oschmann, Numerical study of rope formation and dispersion of non-spherical particles during pneumatic conveying in a pipe bend, Powder Technol. 268 (2014) 219–236.
[35] R. Jasevičius, P. Baltrėnas, R. Kačianauskas, R. Grubliauskas, DEM simulation of the impact of ultrafine glass particles on the partition wall of the multichannel cyclone, Particul. Sci. Tech. 32 (2014) 576–587.
[36] T. Camesano, B. Logan, Probing bacterial electrosteric interactions using atomic force microscopy, Environ. Sci. Technol. 34 (2000) 3354–3362.
[37] J. Tomas, Mechanics of nanoparticle adhesion – a continuum approach, Part. Surf. 8: Detection Adhes. Removal (2003) 1–47.
[38] B.V. Derjaguin, V.M. Muller, Y.P. Toporov, Effect of contact deformations on the adhesion of particles, J. Colloid Interface Sci. 53 (1975) 314–326.
[39] H.-J. Butt, Electrostatic interaction in scanning probe microscopy when imaging in electrolyte solutions, Nanotechnology 3 (1992) 60.
[40] R. Hogg, T.W. Healy, D.W. Fuerstenau, Mutual coagulation of colloidal dispersions, Trans. Faraday Soc. 62 (1966) 1638–1651.
[41] D. Linke, A. Goldman, Bacterial adhesion, Adv. Exp. Med. Biol. 715 (2011) 390.
[42] S. Alexander, Adsorption of chain molecules with a polar head a scaling description, J. Phys. France 38 (1977) 893–987.
[43] P.G. de Gennes, Polymers at an interface; a simplified view, Adv. Colloid Interface Sci. 27 (1987) 189–209.
[44] H.-J. Butt, M. Kappl, H. Mueller, R. Raiteri, Steric forces measured with atomic force microscope at various temperatures, Langmuir 15 (1999) 2559–2565.
[45] H. Rumpf, Die wissenschaft des agglomerierens, Chemie-Ingenieur-Technik, vol. 46, 1974, pp. 1–11.
[46] H. Schubert, Grundlagen des agglomerierens, Chem.-Ing.-Tech. 51 (1979) 266–277.
[47] J. Tomas, Mechanics of Particle Adhesion, Manuscript, Magdeburg, 2008.
[48] X.Q. Feng, H. Li, H.-P. Zhao, S.-W. Yu, Numerical simulations of the normal impact of adhesive microparticles with a rigid substrate, Powder Technol. 189 (2009) 34–41.
[49] B.L. Severson, L.M. Keer, J.M. Ottino, R.Q. Snurr, Mechanical damping using adhesive micro or nano powders, Powder Technol. 191 (2009) 143–148.
[50] E. Sahagún, J. Sáenz, Dissipation by adhesion hysteresis in dynamic force microscopy, Phys. Rev. B 85 (2012) 235412–235415.
[51] M.W. Reeks, J. Reed, D. Hall, On the resuspension of small particles by a turbulent flow, J. Phys. D: Appl. Phys. 21 (1988) 574–589.
[52] A.H. Ibrahim, P.F. Dunn, R.M. Brach, Microparticle detachment from surfaces exposed to turbulent air flow: effects of flow and particle deposition characteristics, J. Aerosol Sci. 35 (2004) 805–821.
[53] T. Paez-Rubio, E. Viau, S. Romero-Hernandez, J. Peccia, Source bioaerosol concentration and rDNA-based identification of microorganisms aerosolized during agricultural wastewater reuse, Appl. Environ. Microbiol. 71 (2005) 804–810.
[54] L.R. Bakken, R.A. Olsen, Buoyant densities and dry-matter contents of microorganisms: conversion of a measured biovolume into biomass, Appl. Environ. Microbiol. 45 (1983) 1188–1195.
[55] H. Jin, X. Huang, Y. Chen, H. Zhao, H. Ye, F. Huang, X. Xing, J. Cai, Photoinactivation effects of hematoporphyrin monomethyl ether on Gram-positive and -negative bacteria detected by atomic force microscopy, Appl. Microbiol. Biotechnol. 88 (2010) 761–770.
[56] A. Touhami, B. Nysten, Y. Dufrene, Nanoscale mapping of the elasticity of microbial cells by atomic force microscopy, Langmuir 19 (2003) 4539–4543.
[57] W.A. Ducker, T.J. Senden, R.M. Pashley, Measurements of forces in liquids using a force microscope, Langmuir 8 (1992) 1831–1836.
[58] J.L. Prince, R.B. Dickinson, Kinetics and forces of adhesion for a pair of capsular/unencapsulated *Staphylococcus mutant* strains, Langmuir 19 (2003) 154–159.
[59] R. Yongsunthon, S.K. Lower, Force measurements between a bacterium and another surface in situ, Adv. Appl. Microbiol. 58 (2006) 97–124.
[60] R. Šimkus, R. Baronas, Ž. Ledas, A multi-cellular network of metabolically active *E. coli* as a weak gel of living Janus particles, Soft Matter 9 (2013) 4489–4500.
[61] R. Jasevicius, J. Tomas, R. Kacianauskas, Simulation of sticking of adhesive particles under normal impact, JVE J. Vibroeng. 11 (2009) 6–17.